Role of the longitudinal piston error in a tiled-grating compressor in second and high-order harmonic generation

**C. Hernández-García · C. Méndez ·
I. Arias · J. R. Vázquez de Aldana ·
O. Varela · I. J. Sola · L. Roso**

Abstract In this work, we study the limitations for overcoming the longitudinal piston error in a femtosecond tiled-grating compressor using nonlinear measurements like second harmonic generation. In particular, we observe the influence of this error when developing high-power laser experiments such as high-order harmonic generation. The generation of nonlinear processes with femtosecond pulses compressed in tiled-grating systems is studied. Special attention is paid to the role of the longitudinal piston error which is the most difficult to overcome in the compressor alignment. A complex spatio-temporal structure is expected to appear due to that misalignment. Both second harmonic generation in nonlinear crystals and high-order harmonic generation in gases are studied and a strong dependence with piston error is found, thus leading to a sub-micron modulation in the generated signal. In particular, the high sensitivity of the high-order harmonics to the longitudinal position allows one to use this processes for the accurate alignment of the compressor to few tens of nanometers.

1 Introduction

Application of the chirped pulse amplification (CPA) technique [1] to the development of high-energy petawatt-class laser systems involves new designs of the compressor stage [2]. The damage threshold of the gratings together with the broad bandwith of femtosecond laser pulses lead to the use of large-section beams and therefore large gratings. Unfortunately, standard gratings are limited in size, and it is very difficult and expensive to make large-size ones. One way to overcome these problems is the application of the grating phasing technique [3], a method that consists of using a mosaic of gratings properly aligned, instead of a monolithic one.

Beside saving costs, the advantage of using the grating phasing technique is the possibility of having as large gratings as desired, just by adding several gratings to the mosaic. Nevertheless, the main disadvantage is the critical alignment of the mosaic, thus obtaining different temporal and spectral laser pulses at the output of the compressor depending on the alignment. Considering a two-phase grating system, one must take into account five degrees of freedom associated to the grating coordinates (x, y, z): tilt (θ_y), tip (θ_x), twist (θ_z), gratings gap (Δx) and longitudinal piston (Δz) (see Fig. 1).

Different techniques based on the spatial far field in the focal plane have succeeded in fixing the alignment of the tilt, tip and twist [4–6]. In order to align the longitudinal piston error, these methods include a 2π indetermination in the phase delay of the beam reflected by the two-phase grating system. Different works overcame this indetermination using interferometric techniques and auxiliary beams [7–11]. Some of the best reported accomplishments have been achieved resolving spectrally the far field [12] leading to a precision in the piston error below $\lambda/10$, being λ the central wavelength of the laser pulse.

In this work, we develop and check a two-grating compressor prototype in which the second grating is a two-phased one. The compressor was tested with the uncompressed output of a 100-fs Ti:Sa laser system (Spectra Physics, 800 nm, 10 Hz

C. Hernández-García (✉) · I. Arias · I. J. Sola
Grupo de Investigación en Óptica Extrema,
Universidad de Salamanca, E-37008 Salamanca, Spain
e-mail: carloshergar@usal.es

C. Méndez · O. Varela · L. Roso
Centro de Láseres Pulsados, CLPU, E-37008 Salamanca, Spain

J. R. Vázquez de Aldana
Grupo de Investigación en Microprocesado de Materiales con
Láser, Universidad de Salamanca, E-37008 Salamanca, Spain

and up to 50 mJ pulse energy) belonging to the laser facility at the University of Salamanca.
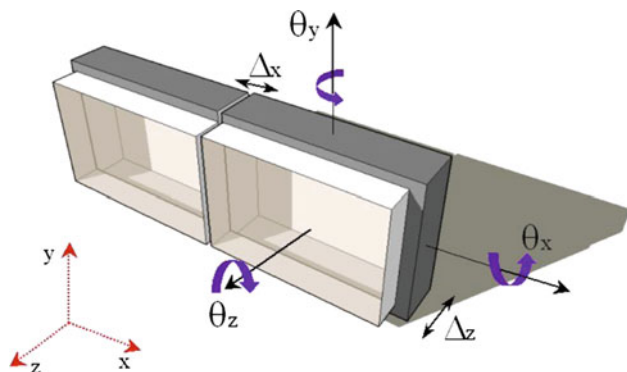
The alignment of the compressor was done using some well-established techniques. The so-generated pulses are used to investigate the role of the longitudinal piston error in experiments of non-linear optics, both second harmonic generation (SHG) in a nonlinear crystal [13] and high-order harmonic generation (HHG) in gases [14–18] are considered here.

2 Tiled-gratings system

2.1 Description of the system

The prototype developed was a two-grating compressor in which the second grating was a two-phased one. The three gratings used in the compressor were 5×5 cm in size, with $1/d = 1,800$ lines/mm, being d the gratings constant. The five degrees of freedom associated to the tiled-grating system (see Fig. 1) must be taken into account in order to properly align the system.

The degrees of freedom involving rotations between the two gratings (tilt, tip and twist) are easily aligned. In our system, they are manually controlled and their alignment is done with two auxiliary CCD cameras placed in the 0-order reflection of the tiled-grating system and in the first one. On the other hand, the alignment of the gratings gap and the longitudinal piston tends to be much more difficult, becoming critical in the nanometer scale. There are two important issues that appear when dealing with those degrees of freedom: (i) the loss of wavelengths—shown in Fig. 2—different for every spatial beam position due to the beam chirp on the tiled grating and due mainly to the gratings gap, but also to the longitudinal piston and (ii) the phase delay between the light reaching each of the gratings. The loss of wavelengths can be minimized when the width

of the spatial beam is much larger than the gratings gap (Δx), or when the two gratings are very close to each other. In the later case, the gratings gap induce a spectral apodization. On the other hand, the phase delay in terms of the longitudinal piston displacement (Δz) is calculated as

$$\Phi_1 - \Phi_2 = k(AB - AC) + \Phi_{\text{grat}} = \frac{2\pi}{\lambda}\Delta z(\cos\theta + \cos\beta) \tag{1}$$
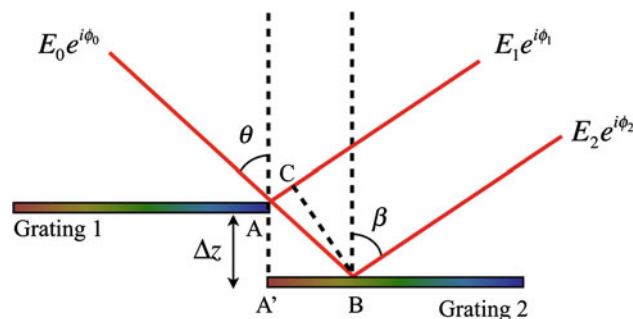
where θ and β are the incidence and diffracted angles on the tiled-grating system, and A, A′, B and C are the points shown in Fig. 3. The third term on Eq. 1, Φ_{grat}, corresponds to the phase delay introduced by the grating between the points A′ and B, and is given by

$$\Phi_{\text{grat}} = \frac{2\pi}{d}A'B \tag{2}$$

A simulation considering both issues was performed in order to guess the temporal shape of the pulse at the output of the compressor. For that purpose, we make an
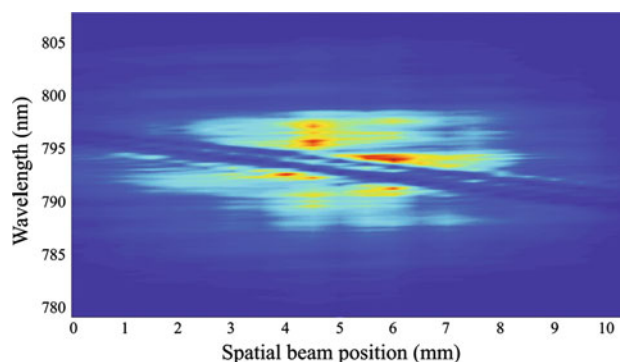
Fig. 2 Spatial variation of the spectrum at the output of the tiled-grating compressor. The measurement was performed along the axis contained in the diffraction plane (*x*-axis). The loss of wavelengths along the spatial beam position can be clearly observed

Fig. 1 Scheme of the five degrees of freedom involved in a two-tiled grating system: tilt (θ_y), tip (θ_x), twist (θ_z), gratings gap (Δx) and longitudinal piston displacement (Δz)

Fig. 3 Scheme of the incident beam reaching the tiled-grating system with an angle θ and being reflected towards a new direction given by the angle β. The reflection on each grating acquires a different phase Φ_1 and Φ_2. The displacement of the piston is represented by $\Delta z = AA'$

approach to the problem considering two pulses with different spectra—as shown in Fig. 4a—then taking into account the two pulses obtained by the diffraction of the incident one in each grating. We introduce a phase delay between the two pulses, thus simulating the longitudinal piston displacement (Δz). Therefore, we are simulating the central part of the spatial beam (see Fig. 2), but note that this behavior would change when considering outer parts of the beam. Figure 4b shows the temporal profile of the pulse in terms of the longitudinal piston displacement. At this point, it is important to distinguish between the phase delay being an even or odd multiple of π, as the temporal profile changes dramatically. If the phase delay is zero or an even multiple of π, the temporal profile is nearly gaussian, but if it is π or an odd multiple of π, the pulse doubles its width, showing a minimum at the center. From Eq. 1, we can extract the periodicity of this behavior, that is given by a displacement of the longitudinal piston of

$$\Delta z = \frac{n\lambda}{2(\cos\theta + \cos\beta)} \quad (3)$$

being n an integer. In our compressor system, in which we use the order of -1 of the diffraction gratings, the incidence angle is $\theta = 50°$, so the piston indetermination is a multiple of Δz approx 0.3 μm, as can be observed in Fig. 4b. For that reason, an extremely high-precision adjustment of the piston is needed, in the nanometer scale. Because it is the difference of being using a nice compressed pulse or a double pulse, this fact can affect dramatically to the experiment. Here it is important to remark the big difference between an aligned or misaligned tiled-grating system in order to achieve the highest intensity in the focal plane. Simulations showed that this effect was present even when the gratings gap (Δx) is negligible.

3 Tiled-grating systems in nonlinear experiments

In our prototype, the gratings gap remains fixed, while the longitudinal piston is motorized by a piezo, whose resolution is 5 nm. Here we define the longitudinal piston delay Δz_d, as the longitudinal piston displacement, where $\Delta z_d = 0$ corresponds to an arbitrary position between the two-tiled gratings in the experiment. In order to roughly align the longitudinal piston, a single-shot autocorrelator was used. Although we were able to clearly distinguish the region where the piston error is compensated, changes in the range of 2π that lead to a behavior close to Fig. 4b are not easily shown using this method. In this section, we present two different nonlinear processes and show how they are affected due to this misalignment.
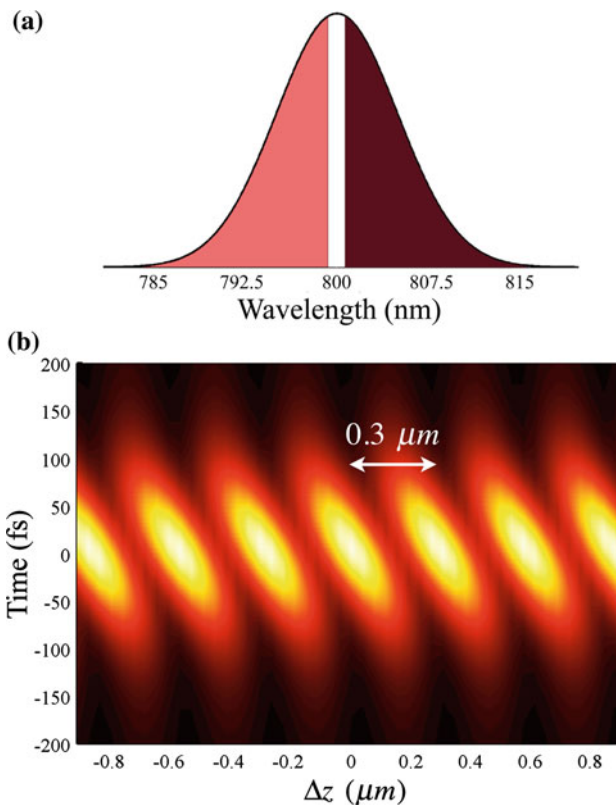

Fig. 4 a Simulated spectrum of the central part of the laser pulse reflected by the tiled-grating system, where an spectral region is removed thus simulating the effect of the gratings gap (Δx). We simulate temporally two gaussian pulses, one with the short wavelength part of the total pulse spectrum (*the lighter one*) and the other with the longer part (*the darker one*). We introduce a phase delay between the two pulses in terms of the longitudinal piston displacement (Δz), thus obtaining the temporal shape of the pulse (**b**)

3.1 Piston effect in SHG

Our first simple analyzed nonlinear process is the second harmonic signal generated by type-I phase matching in a BBO crystal (0.5 mm thick, $\theta_{PM} = 29°$, $\phi_{PM} = 0°$). The spectral acceptance of the crystal is large enough to accommodate the full spectral bandwith (9 nm) of the fundamental pulse. In the experiment, we filtered out the fundamental signal after passing through the BBO crystal. The remaining second harmonic beam was spatially integrated with a 6-cm focal length lens and detected in a fiber spectrometer. The core of the fiber was 5 μm in diameter.

Figure 5a shows the measured pulse spectrum versus the longitudinal piston delay. First of all, we can clearly identify a cut in the spectrum near the horizontal axis borders of the figure due to the loss of wavelengths caused by the piston misalignment. The nonlinear process amplifies this effect and helps to maintain the system near the region in which the second harmonic signal is maximum and the spectrum is close to gaussian shape. Let's note here
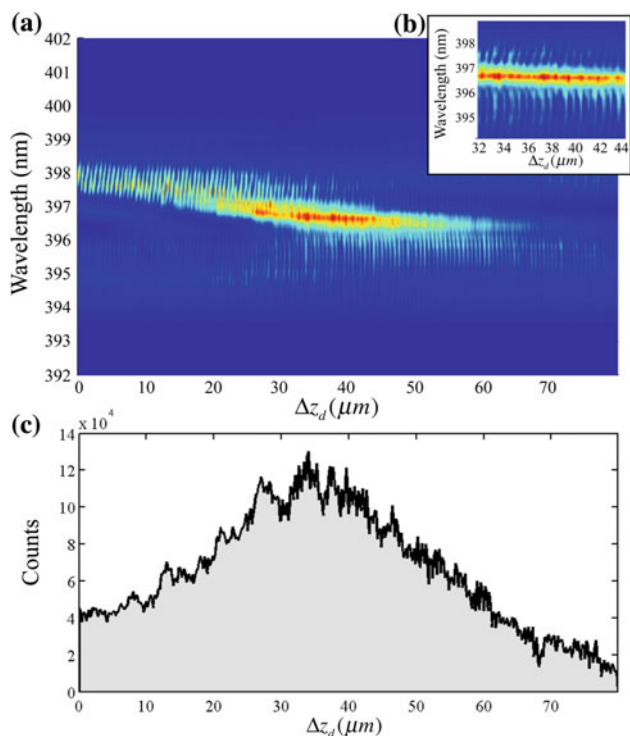
Fig. 5 a Spectrum of the second harmonic signal versus the longitudinal piston delay (Δz_d), b magnification of the central region, and c its integration over the wavelength. We can see a region in which the amount of signal is maximum, that is, the system is closer to be perfectly aligned. Moreover, we can clearly see the fringes separated ~ 0.3 μm corresponding to the 2π piston indetermination predicted by Eq. 3. Note that $\Delta z_d = 0$ corresponds to an arbitrary position between the two-tiled gratings in the experiment.

that in this case, the nonlinear process corrects somehow the loss of wavelengths that could be observed in the output fundamental beam (Fig. 2). Moreover, if we integrate the signal over the wavelength (see Fig. 5c), we observe a position of the piston where the signal is maximum, thus, giving us information about the position in which the system is best aligned. On the other hand, in Fig. 5b, we can also observe the periodic ~ 0.3 μm structure corresponding to the 2π piston indetermination predicted by Eq. 3. The figure shows maxima and minima in the second harmonic signal, corresponding to the $\pi - 2\pi$ piston displacement, in agreement to what was shown in Fig. 4b. This analysis gives us the first idea of the importance of considering the piston alignment when triggering nonlinear optical processes and gives information for the correct alignment of the tiled-grating system.

3.2 Piston effect in HHG

The next analyzed nonlinear process is the variation of the HHG spectrum with the longitudinal piston delay. Odd harmonics of the fundamental frequency are generated by
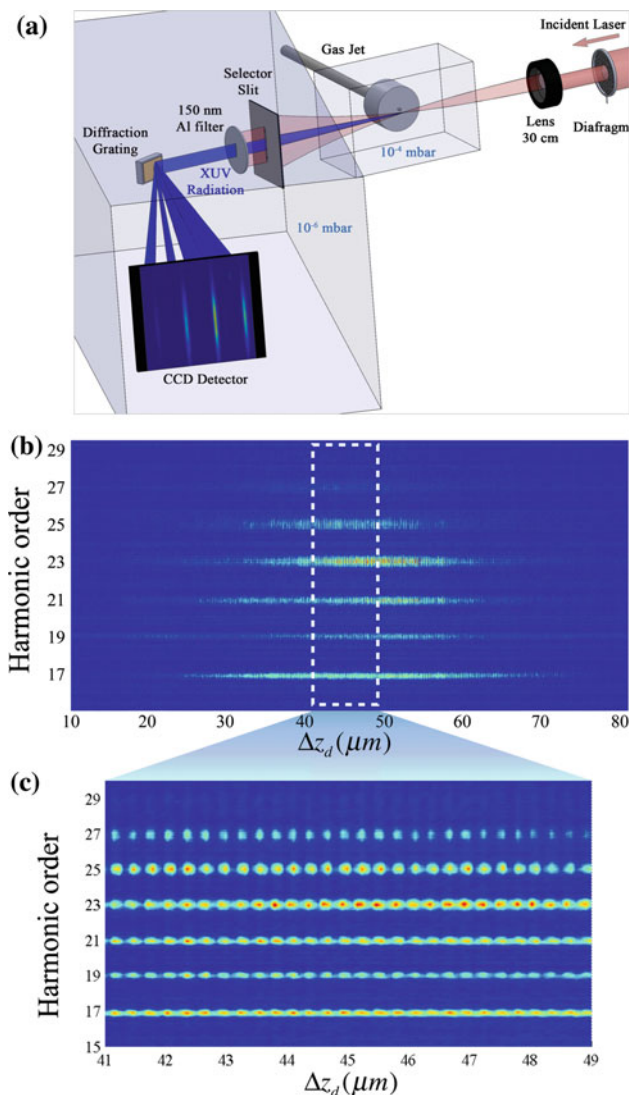
Fig. 6 a Scheme of the experimental setup used for HHG generation. A diaphragm is placed before the focusing lens (30-cm focal length) in order to create an aperture in the laser beam and optimize phase-matching conditions. XUV radiation is generated in an argon gas jet exiting from a 500-μm nozzle inside a vacuum chamber (10^{-4} mbar) whereas the remaining infrared laser pulse is eliminated by a 150-nm thick Al filter. The harmonics are spatially and spectrally characterized by a Rowland circle type XUV spectrometer inside another vacuum chamber (10^{-6} mbar). In b, we show the spectrum of the high-order harmonic signal (from harmonic 17th to 27th) versus the longitudinal piston delay (Δz_d). We can observe that the intensity and number of generated harmonics tend to be maximum at the center of the figure. c is a zoom of b, where we can see the periodic structure of ~ 0.3 μm due to the phase delay introduced by the piston delay. Note that $\Delta z_d = 0$ corresponds to an arbitrary position between the two-tiled gratings in the experiment.

focusing the compressed laser beam with a 30-cm focal length lens into a pulsed argon jet exiting from a 500 μm nozzle inside a vacuum chamber (10^{-4} mbar). The relative distance between the focus position and gas jet was optimized to favor phase matching conditions [19, 20].

Moreover, the incident laser beam was apertured before being focused in order to reduce the Gouy mismatch contribution [21]. Once the XUV radiation was generated, a thin aluminium filter (150 nm in thickness) was used to eliminate the remaining infrared laser pulse. In the next step, the harmonics were spatially selected by a slit before being characterized by a Rowland circle-type XUV spectrometer (McPherson 248/310G) [22, 23]. The spectrometer consists of a reflective spherical grating, a microchannel plate coupled to phosphore screen and a CCD detector, all of them inside a vacuum chamber (10^{-6} mbar). In our measurements, the XUV radiation was spatially integrated in the CCD detector. Figure 6a represents a scheme of the setup used in the experiment.

The most relevant result of this paper is presented in Fig. 6b and c, where we show the variation of the HHG spectrum with the longitudinal piston delay. The analysis of the generated spectrum indicates that there are two main issues related to the alignment of the piston. Firstly, we observe that varying the piston delay, there is a region in which the intensity of the harmonics is higher, so we expect to have the piston correctly aligned in that region. Secondly, the number of harmonics generated is also maximum in that region, where the cut-off is shifted toward higher frequencies. Figure 6c is a zoom of Fig. 6b, where we can again observe the periodic structure of ~ 0.3 μm due to the 2π indetermination predicted by Eq. 3. These results show clearly how important is the piston alignment for these kind of experiments, as HHG process is very sensitive to both the intensity and the temporal shape of the incident laser pulse. An error of some tens of nanometers in the piston alignment can lead to a weaker signal and even no HHG signal if it is close to 100 nm. Therefore, this method allows us to place the tiled-grating system in the region where the piston delay influence to the laser pulse is lower, by observing the intensity and the number of harmonics generated.

4 Conclusions

A prototype compressor based on the phasing grating technique was implemented for a 100-fs Ti:Sa laser system (Spectra Physics, 800 nm, 10 Hz up to 50 mJ). We have tested the effect of the piston misalignment between the tiled gratings causes in high-power nonlinear processes. In particular, the effect in the SHG process in a BBO crystal allows us to partially correct the effect of the gratings gap in the spectrum of the fundamental beam as well as provides a simple method for an initial alignment of the longitudinal piston. The second tested process is HHG generation, which could also be used as a method to discriminate the correct

position of the piston term. Experimental results show that although we do not know the exact position of the piston alignment, we are able to place the system optimized for our experiment, avoiding the effect of the π-phase delay introduced by the piston displacement. This accuracy should be taken into account when using the pulses generated by these compressors for high-power laser applications.

References

1. D. Strickland, G. Mourou, Opt. Commun. **56**, 219–221 (1985)
2. S. Backus, C.G. Durfee III, M.M. Murnane, H.C. Kapteyn, Rev. Sci. Instrum. **69**, 1207 (1998)
3. T. Zhang, M. Yonemura, Y. Kato, Opt. Commun. **145**, 367–376 (1998)
4. T.J. Kessler, J. Bunkenburg, H. Huang, A. Koslov, D. Meyerhofer, Opt. Lett. **29**, 635 (2004)
5. A. Cotel, M. Castaing, P. Pichon, C. Le Blanc, Opt. Exp. **33**, 2742 (2007)
6. A. Cotel, C. Crotti, P. Audebert, C. Le Bris, C. Le Blanc, Opt. Lett. **32**, 1749 (2007)
7. S. Mousset, C. Rouyer, G. Marre, N. Blanchot, S. Montant, B. Wattellier, Opt. Lett. **31**, 2634 (2006)
8. Y. Hu, L. Zeng, L. Li, Opt. Commun. **269**, 285 (2007)
9. X. Ma, J. Zhu, Chin. Opt. Lett. **5**, 25 (2007)
10. Y. Zuo, X. Wei, X. Wang, Q. Zhu, R. Ren, Z. Huang, H. Liu, Opt. Lett. **3**, 280 (2007)
11. J. Qiao, A. Kalb, T. Nguyen, J. Bukenburg, D. Canning, J.H. Kelly, Opt. Lett. **33**, 1684 (2007)
12. M. Hornung, R. Bödefeld, A. Kessler, J. Hein, M.C. Kaluza, Opt. Lett. **35**, 2073 (2010)
13. P.A. Franken, A.E. Hill, C.W. Peters, G. Weinreich, Phys. Rev. Lett. **7**, 118–119 (1961)
14. M. Ferray, A. L'Huillier, X.F. Li, L.A. Lompre, G. Mainfray, C. Manus, J. Phys. B **21**, L31–L35 (1988)
15. J.L. Krause, K.J. Schafer, K.C. Kulander, Phys. Rev. Lett. **68**, 3535–3538 (1992)
16. P. Agostini, L.F. DiMauro, Rep. Prog. Phys. **67**, 813–855 (2004)
17. P. Corkum, F. Krausz, Nat. Phys. **3**, 381–387 (2007)
18. T. Popmintchev, M. Chen, P. Arpin, M.M. Murnane, H.C. Kapteyn, Nat Photonics **4**, 822–832 (2010)
19. P. Salières, A. LHuillier, M. Lewenstein: Phys. Rev. Lett. **74**, 3776 (1995)
20. C. Hernández-García, J.A. Pérez-Hernández, J. Ramos, E. Conejero Jarque, L. Roso, L. Plaja, Phys. Rev. A **82**, 033432 (2010)
21. S. Kazamias, F. Weihe, D. Douillet, C. Valentin, T. Planchon, S. Sebban, G. Grillon, F. Augé, D. Hulin, Ph Balcou, Eur. Phys. J. D **21**, 353–359 (2002)
22. J.L. Schwob, A.W. Wouters, S. Suckewer, M. Finkenthal, Rev. Sci. Instrum. **58**, 1601–1615 (1987)
23. B.J. MacGowan, J.A. Koch, S. Mrowka, Rev. Sci. Instrum. **63**, 5122–5123 (1992)